

# RDGCL: Reaction-Diffusion Graph Contrastive Learning for Recommendation

Jeongwhan Choi<sup>\*1</sup>, Hyowon Wi<sup>\*2</sup>, Chaejeong Lee<sup>1</sup>, Sung-Bae Cho<sup>1</sup>, Dongha Lee<sup>1</sup>, Noseong Park<sup>2†</sup>

<sup>1</sup>Yonsei University, Seoul, South Korea

<sup>2</sup>KAIST, Daejeon, South Korea

{jeongwhan.choi, chaejeong\_lee, sbcho, donalee}@yonsei.ac.kr, {hyowon.wi, noseong}@kaist.ac.kr

## Abstract

Contrastive learning (CL) has emerged as a promising technique for improving recommender systems, addressing the challenge of data sparsity by using self-supervised signals from raw data. Integration of CL with graph convolutional network (GCN)-based collaborative filterings (CFs) has been explored in recommender systems. However, current CL-based recommendation models heavily rely on low-pass filters and graph augmentations. In this paper, inspired by the reaction-diffusion equation, we propose a novel CL method for recommender systems called the reaction-diffusion graph contrastive learning model (RDGCL). We design our own GCN for CF based on the equations of diffusion, i.e., low-pass filter, and reaction, i.e., high-pass filter. Our proposed CL-based training occurs between reaction and diffusion-based embeddings, so there is no need for graph augmentations. Experimental evaluation on 5 benchmark datasets demonstrates that our proposed method outperforms state-of-the-art CL-based recommendation models. By enhancing recommendation accuracy and diversity, our method brings an advancement in CL for recommender systems.

## 1 Introduction

CL is attracting much attention and is being actively researched in the field of machine learning (Jaiswal et al. 2020; Khosla et al. 2020; Liu et al. 2021b; Chen, Luo, and Li 2021). CL enhances the user/item embedding process with the learning representation principle, which increases the similarity between positive pairs and maximizes the dissimilarity between negative pairs. CL has achieved many successes in a variety of domains, including computer vision (Chen et al. 2020b,c; He et al. 2020a), natural language processing (Radford et al. 2021; Chuang et al. 2022; Bayer, Kaufhold, and Reuter 2022) and graph data (Qiu et al. 2020; Hassani and Khasahmadi 2020; Zhu et al. 2021, 2020). In the field of recommender systems, recent CF methods are mostly based on it (Wu et al. 2021; Yu et al. 2022b,a; Cai et al. 2023; Xu et al. 2023; Li et al. 2023; Jing et al. 2023).

The integration of CL with GCNs has great potential in tackling the data sparsity problem in recommender systems (Wu et al. 2021; Jing et al. 2023). GCN-based CF methods excel at capturing complex dependencies and interac-

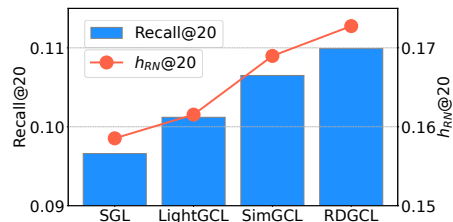


Figure 1: Comparison in terms of Recall@20 and  $h_{RN}@20$ , the harmonic mean of the recall and novelty (see Sec. 4), on Yelp. Our RDGCL outperforms SGL (Wu et al. 2021), SimGCL (Xu et al. 2023), and LightGCL (Cai et al. 2023).

Model	View generation	Low-pass filter	High-pass filter
SGL	Node/edge dropout	✓	✗
SimGCL	Injecting noises into embs.	✓	✗
LightGCL	Filtering graphs with SVD	✓	✗
<b>RDGCL</b>	Low vs. High-pass embs.	Diffusion eq.	Reaction eq.

Table 1: Comparison of existing CL-based methods that differ at three points: i) how to generate views for CF, ii) using low-pass filters, and iii) using high-pass filters.

tions among entities in graph-structured data, making them suitable for modeling user-item interactions (Wang et al. 2019; Lee, Kim, and Lee 2018; He et al. 2020b; Mao et al. 2021a,b; Choi, Jeon, and Park 2021; Shen et al. 2021; Hu et al. 2022; Chen et al. 2020a; Kong et al. 2022; Hong et al. 2022; Fan et al. 2022; Liu et al. 2021a). However, the inherent data sparsity in recommendation scenarios, where most users interact with only a few items, pose a challenge. CL addresses this by exposing the model to more diverse training environments, thereby stabilizing the training process and mitigating overfitting.

Existing CL-based recommendation models rely on graph augmentation techniques to generate contrastive views. These techniques typically involve perturbing graph structures or adding noise to node embeddings. As in Table 1, SGL (Wu et al. 2021) perturbs graph structures, SimGCL (Yu et al. 2022b) injects uniform noise into embeddings, and LightGCL (Cai et al. 2023) reconstructs graph

<sup>\*</sup>These authors contributed equally.

<sup>†</sup>Noseong Park is the corresponding author.

structures through singular value decomposition (SVD). However, the current paradigm of CL-based CF has several limitations:

1. Graph augmentations can introduce noise and redundancies, potentially degrading the quality of the learned node representation.
2. These augmentations may not generate sufficient diversity and contrast in node representations (see Fig. 1).
3. Existing methods using LightGCN use low-pass graph filters (see Table 1), overlooking the importance of high-pass filters.

Recent research has highlighted the limitations of using only low-frequency signals (i.e., popular items) (Peng, Sugiyama, and Mine 2022; Choi et al. 2023a; Du et al. 2023) in recommender systems. Models based on low-pass filters, such as LightGCN struggle to recommend novel or diverse items that reflect unique user preferences.

To address these limitations, the key design points in our proposed method are twofold: i) a new GCN-based network is proposed for CF, and ii) a new CL method for it is designed. Our method with the two contributions is called *reaction-diffusion graph contrastive learning* (RDGCL) since those design points are greatly inspired by the reaction-diffusion equation.

Our approach uses the reaction-diffusion equation in the context of GCNs, where the diffusion equation makes the embeddings of neighboring nodes similar (Wang et al. 2021), and the reaction equation makes them dissimilar (high-pass filter) (Choi et al. 2023b; Wang et al. 2023). In the perspective of graph signal processing, the diffusion (resp. reaction) equation corresponds to the low-pass (resp. high-pass) filter.

RDGCL differs from other CL-based CF methods by using a *single pass* architecture. For instance, LightGCL has two GCN instances, one for the main CF task and the other for the augmented graph view purpose, which we call *two passes*. Since RDGCL has both diffusion and reaction layers internally, this allows for efficient CL training between these layers without the need for separate graph augmentation steps (see Fig. 3).

This paper presents a comprehensive evaluation of RDGCL using 5 benchmark datasets and 14 baselines. Our experimental results demonstrate the superiority of RDGCL in terms of recommendation accuracy, coverage, and novelty. The main contributions of this paper are:

- We propose RDGCL, a novel CL-based CF approach incorporating both diffusion (low-pass filtering) and reaction (high-pass filtering) equations in its neural network design and CL training method.
- To our knowledge, RDGCL is the first to apply the reaction-diffusion equation for CL-based CF methods.
- RDGCL outperforms 14 baselines on 5 benchmark datasets.
- In terms of relevance and diversity metrics (e.g. coverage and novelty), RDGCL achieves the most balanced performance, recommending more diverse and novel items while maintaining high accuracy (see Fig. 1).

## 2 Preliminaries & Related Work

### Graph Filters and GCN-based CFs

Let  $\mathbf{R} \in \{0, 1\}^{|\mathcal{U}| \times |\mathcal{V}|}$  be an interaction matrix, where  $\mathcal{U}$  and  $\mathcal{V}$  is sets of users and items.  $\mathbf{R}_{u,v} = 1$  iff an interaction  $(u, v)$  is observed and 0 otherwise. The adjacency matrix  $\mathbf{A} \in \mathbb{R}^{N \times N}$ , where  $N = |\mathcal{U}| + |\mathcal{V}|$ , represent the graph structure. The Laplacian matrix is defined as  $\mathbf{L} = \mathbf{D} - \mathbf{A} \in \mathbb{R}^{N \times N}$ , with  $\mathbf{D}$  being the diagonal degree matrix. The symmetric normalized adjacency and Laplacian matrices are defined as  $\tilde{\mathbf{A}} = \bar{\mathbf{D}}^{-\frac{1}{2}} \mathbf{A} \bar{\mathbf{D}}^{-\frac{1}{2}}$ , and  $\tilde{\mathbf{L}} = \mathbf{I} - \tilde{\mathbf{A}}$ , where  $\bar{\mathbf{D}} = \mathbf{D} + \mathbf{I}$  and  $\bar{\mathbf{A}} = \mathbf{A} + \mathbf{I}$ .

The operation  $\tilde{\mathbf{L}}\mathbf{x}$  can be interpreted as a filter that modifies the frequency components of the graph signal  $\mathbf{x}$  (Chung 1997). The Laplacian filter enhances signal components associated with higher eigenvalues  $\gamma_i \in (1, 2)$  while reducing those with lower eigenvalues  $\gamma_i \in [0, 1]$ . This behavior characterizes Laplacian matrices as high-pass filters, emphasizing differences in node features (Ekambaram 2013). In contrast, normalized adjacency matrices function as low-pass filters (Nt and Maehara 2019), reducing non-smooth signal components. This is due to all eigenvalues of the adjacency matrices being less than 1, i.e.  $\gamma_i \in (-1, 1]$ .

Most GCN-based CF approaches, including LightGCN (He et al. 2020b), use low-pass filters to enhance the smoothness of node representations. While some recent studies use high-pass filters (Peng, Sugiyama, and Mine 2022; Choi et al. 2023a; Shin et al. 2023), their application in generating views for CL in recommendation remains unexplored. Our key idea is to apply high-pass graph filters in the CL framework for recommendation.

### Contrastive Learning for Recommendation

Deep learning-based recommender systems have shown remarkable performance in recent years. However, they suffer from data sparsity and cold start problems, since they rely heavily on labels, i.e., positive user-item interactions (Yu et al. 2018; You et al. 2020). To address these problems, self-supervised methods, particularly CL-based CF methods (Jing et al. 2023; Wu et al. 2021) have emerged as promising outcomes.

SGL (Wu et al. 2021) first applied the CL to graph-based recommendation, using LightGCN (He et al. 2020b) as its graph encoder. It introduces three operators to generate augmented views: node dropouts, edge dropouts, and random walks. By contrasting these augmented views, it improves the recommendation accuracy, especially for long-tail items, and the robustness against interaction noises. For CL, InfoNCE (Oord, Li, and Vinyals 2018) is defined as follows:

$$\mathcal{L}_{CL} = \sum_{i \in \mathcal{B}} -\log \frac{\exp(\text{sim}(\mathbf{e}'_i, \mathbf{e}''_i)/\tau)}{\sum_{j \in \mathcal{B}} \exp(\text{sim}(\mathbf{e}'_i, \mathbf{e}''_j)/\tau)}, \quad (1)$$

where  $i, j$  are a user and an item in a mini-batch  $\mathcal{B}$  respectively,  $\text{sim}(\cdot)$  is the cosine similarity,  $\tau$  is the temperature, and  $\mathbf{e}'$ ,  $\mathbf{e}''$  are augmented node representations. The CL loss increases the alignment between  $\mathbf{e}'_i$  and  $\mathbf{e}''_i$  nodes, viewing the representations of the same node  $i$  as positive pairs. Simultaneously, it minimizes the alignment between the node

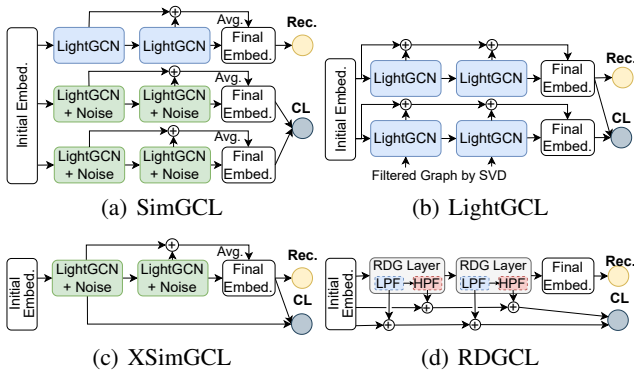


Figure 2: The architectures of SimGCL, LightGCL, XSimGCL, and RDGCL.

representations of  $\mathbf{e}'_i$  and  $\mathbf{e}''_j$ , viewing the representations of the different nodes  $i$  and  $j$  as negative pairs.

SimGCL (Yu et al. 2022b) simplifies the graph augmentation process for its CL by perturbing node representations with random noise. XSimGCL (Yu et al. 2022a) replaces the final-layer CL of SimGCL with a cross-layer CL approach — our RDGCL also follows this cross-layer CL approach. It only uses one GCN-based encoder and contrasts the embeddings of different layers, and this cross-layer CL reduces the computational complexity since it has only one neural network. NCL (Lin et al. 2022) does not change the existing graph structure to create contrastive views and finds the neighbors of a user or item in semantic space to suggest new contrastive learning. NCL incorporates semantic neighbors into the prototype-contrastive objective to find potential neighbor relationships in semantic space. LightGCL (Cai et al. 2023) proposes a SVD-based graph augmentation strategy to effectively distill global collaborative signals. In specific, SVD is first performed on the adjacency matrix. Then, the list of singular values is truncated to retain the largest values, i.e., the ideal low-pass filter, and then its truncated matrix is used to purify the adjacency matrix. As shown in Fig. 2, existing CL-based recommender systems are limited to low-pass filters since i) their backbones are mostly LightGCN and ii) they augment views with low-pass filters.

### Reaction-Diffusion Equations

Reaction-diffusion equations are partial differential equations that describe how the concentration of substances distributed in space changes under the influence of local chemical reactions and diffusion (Turing 1952; Kondo and Miura 2010). A general form of a reaction-diffusion equation is:

$$\frac{\partial u}{\partial t} = \nabla^2 u + R(u), \quad (2)$$

where  $u(x, t)$  is the concentration of a substance at position  $x$  and time  $t$ ,  $\nabla^2$  is the Laplace operator, and  $R(u)$  is the reaction term. There are different types of reaction terms to describe pattern formation phenomena in various biological (Fisher 1937) and chemical (Allen and Cahn 1979; Pinar 2021) systems, and image processing (Turk 1991; Witkin

and Kass 1991; Plonka and Ma 2008; Chen and Pock 2016). On graphs, reaction-diffusion equations can be discretized using finite difference methods. Using the Euler scheme, we can approximate the reaction-diffusion equation in the context of graph signal processing as:

$$u(t + \Delta t) = u(t) + \Delta t(-\tilde{\mathbf{L}}u(t) + R(u(t))), \quad (3)$$

where  $\Delta t$  is the time step size and  $u(t) \in \mathbb{R}^N$  is the graph signal at time  $t$ . This equation updates the graph signal by applying diffusion and reaction terms at each time step.

Inspired by reaction-diffusion filters in image processing that iterate between blurring (low-pass) and sharpening (high-pass) processes (Plonka and Ma 2008), we use graph high-pass filters to design the interaction of nodes in the reaction term.

### Neural Ordinary Differential Equations

Neural ordinary differential equations (NODEs) (Chen et al. 2018) solve the initial value problem to calculate  $\mathbf{h}(t_{i+1})$  from  $\mathbf{h}(t_i)$ :

$$\mathbf{h}(t_{i+1}) = \mathbf{h}(t_i) + \int_{t_i}^{t_{i+1}} f(\mathbf{h}(t), t; \theta_f) dt, \quad (4)$$

where  $f(\cdot)$ , parameterized by  $\theta_f$ , approximates the time-derivative of  $\mathbf{h}$ . Various ODE solvers can be used, with the Euler method being a simple example:

$$\mathbf{h}(t + s) = \mathbf{h}(t) + s \cdot f(\mathbf{h}(t)), \quad (5)$$

where  $s$  is the step size. Eq. (5) is identical to a residual connection when  $s = 1$  and therefore NODEs are a continuous generalization of residual networks.

Continuous GCNs (Xhonneux, Qu, and Tang 2020; Poli et al. 2019) use NODEs to transform discrete GCN layers into continuous layers, which can be interpreted in terms of diffusion processes (Wang et al. 2021; Chamberlain et al. 2021). Since our goal is to design our method to bring the reaction-diffusion process into a GCN and CL-based recommender system, we design our method based on NODEs.

## 3 Proposed Method

### Overall Architecture

Our RDGCL architecture, shown in Fig. 3 begins with an initial embedding  $\mathbf{E}(0)$  that evolves over time  $t \in [0, T]$  through a reaction-diffusion graph (RDG) layer. This embedding evolutionary process is described by:

$$\mathbf{E}(T) = \mathbf{E}(0) + \int_0^T f(\mathbf{E}(t)) dt, \quad (6)$$

where  $\mathbf{E}(t) \in \mathbb{R}^{N \times D}$  is the node embedding matrix at time  $t$  with  $D$  dimensions.  $f(\mathbf{E}(t))$  is a RDG layer which outputs  $\frac{d\mathbf{E}(t)}{dt}$ . The iterative process of the RDG layer consists of:

1. The RDG layer applies a low-pass filter (e.g., a diffusion process) to  $\mathbf{E}(t_i)$  to derive its low-pass filtered embedding  $\mathbf{B}(t_i)$ .
2. It then applies a high-pass filter (e.g., a reaction process) to  $\mathbf{B}(t_i)$  to derive  $\mathbf{E}(t_{i+1})$ .

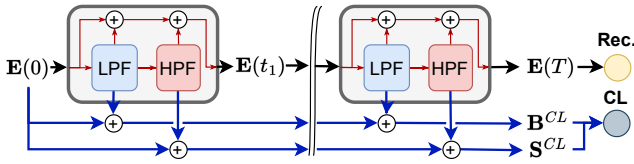


Figure 3: The illustration of our RDGCL where we solve our reaction-diffusion system with the Euler method. LPF (resp. HPF) stands for the low (resp. high)-pass filter.

RDGCL uses  $\mathbf{E}(T)$  for recommendation while contrasting two views,  $\mathbf{B}^{CL}$  and  $\mathbf{S}^{CL}$ , representing low-pass and high-pass information respectively. This approach is called *cross-layer CL* or *single-pass CL*.

### Reaction-Diffusion Graph (RDG) Layer

Our RDG layer is defined by:

$$f(\mathbf{E}(t)) := \frac{d\mathbf{E}(t)}{dt} = -\tilde{\mathbf{L}}\mathbf{E}(t) + \alpha R(\mathbf{E}(t)), \quad (7)$$

where  $R(\cdot)$  is the reaction term, and  $\alpha$  is the reaction rate coefficient to (de-)emphasize the reaction term.

**Diffusion Process as Low-pass Filter** Multiplying with the adjacency matrix ( $\mathbf{A}$  or  $\tilde{\mathbf{A}}$ ) is considered a low-pass filtering operation. Many GCNs can be generalized to diffusion process (Wang et al. 2021; Chamberlain et al. 2021):

$$\mathbf{B}(t) = \mathbf{E}(t) - \tilde{\mathbf{L}}\mathbf{E}(t) = \mathbf{E}(t) + (\tilde{\mathbf{A}} - \mathbf{I})\mathbf{E}(t) = \tilde{\mathbf{A}}\mathbf{E}(t). \quad (8)$$

**Reaction Process as High-pass Filter** The reaction process acting as a high-pass filter, is applied to  $\mathbf{B}(t)$ :

$$R(\mathbf{E}(t)) := \tilde{\mathbf{L}}\mathbf{B}(t) = \tilde{\mathbf{L}}\tilde{\mathbf{A}}\mathbf{E}(t). \quad (9)$$

The reaction process counteracts the oversmoothing effect in GCNs. Oversmoothing tends to standardize user preferences towards popular items, worsening the long-tail problem (Zhao et al. 2022; Zhou et al. 2023). RDGCL emphasizes the distinctions among nodes by including high-pass filtering, thereby recommending long-tail items to users. In Sec. 4 and Sec. 4, we will provide empirical evidence of the high-pass filter’s effectiveness in promoting diversity and alleviating the popularity bias.

### Cross-layer Contrastive Learning

We extract low-pass (or diffusion) and high-pass (or reaction) views from Eq. (7) along  $[0, T]$ :

$$\mathbf{B}^{CL} = \mathbf{E}(0) + \sum_{i=1}^K \mathbf{B}(t_i), \quad \mathbf{S}^{CL} = \mathbf{E}(0) + \sum_{i=1}^K R(\mathbf{E}(t_i)), \quad (10)$$

where we solve Eq. (6) via  $K$  steps with an ODE solver.

We perform the CL training by directly contrasting two views of reaction and diffusion using InfoNCE loss:

$$\mathcal{L}_{CL} = \sum_{i \in \mathcal{B}} -\log \frac{\exp(\text{sim}(\mathbf{b}_i^{CL}, \mathbf{s}_i^{CL})/\tau)}{\sum_{j \in \mathcal{B}} \exp(\text{sim}(\mathbf{b}_i^{CL}, \mathbf{s}_j^{CL})/\tau)}, \quad (11)$$

Component	LightGCN	SGL	SimGCL	RDGCL
Adj. Matrix	$\mathcal{O}(2 \mathbf{A} )$	$\mathcal{O}((2+4\rho) \mathbf{A} )$	$\mathcal{O}(2 \mathbf{A} )$	$\mathcal{O}(2 \mathbf{A} )$
GCN	$\mathcal{O}(2 \mathbf{A} KD)$	$\mathcal{O}((2+4\rho) \mathbf{A} KD)$	$\mathcal{O}(6 \mathbf{A} KD)$	$\mathcal{O}(4 \mathbf{A} KD)$
CL	N/A	$\mathcal{O}( \mathcal{B} MD)$	$\mathcal{O}( \mathcal{B} MD)$	$\mathcal{O}( \mathcal{B} MD)$

Table 2: The comparison of analytical time complexity

where  $\mathbf{b}_i^{CL}$ ,  $\mathbf{s}_i^{CL}$ , and  $\mathbf{s}_j^{CL}$  are node representations from Eq. (10). The final objective function is as follows:

$$\mathcal{L} = \mathcal{L}_{BPR} + \lambda_1 \cdot \mathcal{L}_{CL} + \lambda_2 \cdot \|\Theta\|_2^2, \quad (12)$$

where  $\mathcal{L}_{BPR}$  is the Bayesian personalized ranking (BPR) loss and  $\Theta = \mathbf{E}(0)$ .

### Model Complexity

We analyze the time complexity of RDGCL compared to LightGCN, SGL, and SimGCL. Let  $|\mathbf{A}|$  be the number of edges,  $|\mathcal{B}|$  the batch size,  $M$  the number of nodes in a batch,  $K$  the number of layers or ODE steps, and  $\rho$  the edge keeping-rate in SGL. Table 2 summarizes the time complexity which gives the following findings:

- RDGCL, LightGCN and SimGCL, requires  $\mathcal{O}(2|\mathbf{A}|)$  to construct the adjacency matrix, while SGL needs nearly triple this cost due to graph augmentation.
- The computational cost per step of RDGCL is lower than that of SGL, requiring only two matrix multiplication operations in Eq. (7).
- For the CL loss computation, the complexity of RDGCL is the same as those of other models, which is  $\mathcal{O}(|\mathcal{B}|D + |\mathcal{B}|MD)$ , where  $\mathcal{O}(|\mathcal{B}|D)$  and  $\mathcal{O}(|\mathcal{B}|MD)$  are for positive and negative views, respectively. For brevity, we show it as  $\mathcal{O}(|\mathcal{B}|MD)$ .

This analysis shows the computational efficiency of RDGCL relative to existing methods.

### Property of RDG Layer

Under Euler discretization with  $dt = 1$ ,  $T = 1$ , and  $\alpha = 1$ , Eq. (6) can be interpreted as applying a  $2\tilde{\mathbf{A}} - \tilde{\mathbf{A}}^2$  filter to  $\mathbf{E}(t)$ . The derivation of this filter is provided in *Appendix A*.

**Theorem 1.** *The RDG layer applies a  $2\tilde{\mathbf{A}} - \tilde{\mathbf{A}}^2$  filter, which emphasizes mid-to-high frequency components of the graph signal more than the  $\tilde{\mathbf{A}}$  filter.*

This filter emphasizes higher-frequency signals while attenuating low-frequency ones (Singer, Shkolnisky, and Nadler 2009), unlike the  $\tilde{\mathbf{A}}$  filter. This property captures unique user preferences, potentially increasing recommendation diversity (see Sec.4). The proof is in *Appendix B*.

### Relation to Other Methods

RDGCL uses a *single pass* for CL and CF tasks, in contrast to SimGCL and LightGCL, which use separate passes. This approach improves efficiency and consistency in representation learning. While XSimGCL shares similarities with RDGCL in using a single-pass, cross-layer CL method, it remains limited to low-pass filters. RDGCL adopts the



Data	Metric	LightGCN	LT-OCF	HMLET	SGL	SimGRACE	GCA	HCCF	SHT	SimGCL	XSimGCL	NCL	LightGCL	GF-CF	BSPM	RDGCL	Imp.
Yelp	Recall@20	0.0826	0.0947	0.0859	0.0967	0.0899	0.0779	0.0995	0.0853	<b>0.1065</b>	0.0974	0.0956	0.1012	0.1043	<b>0.1059</b>	<b>0.1099</b>	3.19%
	NDCG@20	0.0690	0.0800	0.0699	0.0824	0.0775	0.0670	0.0842	0.0719	<b>0.0912</b>	0.0823	0.0812	0.0870	0.0890	<b>0.0913</b>	<b>0.0939</b>	2.77%
	Recall@40	0.1346	0.1531	0.1388	0.1544	0.1443	0.1279	0.1578	0.1382	<b>0.1688</b>	0.1564	0.1522	0.1591	0.1659	<b>0.1677</b>	<b>0.1721</b>	1.95%
	NDCG@40	0.0882	0.1016	0.0898	0.1032	0.1032	0.0851	0.1056	0.0913	0.1038	0.1040	0.1019	0.1081	<b>0.1115</b>	<b>0.1139</b>	<b>0.1165</b>	2.28%
Gowalla	Recall@20	0.1294	0.2215	0.2157	<b>0.2410</b>	0.1519	0.1899	0.2222	0.1877	0.2382	0.2314	0.1933	0.2351	0.2347	<b>0.2455</b>	<b>0.2564</b>	4.43%
	NDCG@20	0.0781	0.1287	0.1270	<b>0.1427</b>	0.0850	0.1100	0.1298	0.1119	0.1412	0.1380	0.1129	0.1386	0.1382	<b>0.1472</b>	<b>0.1549</b>	5.19%
	Recall@40	0.1869	0.3131	0.3010	<b>0.3313</b>	0.2225	0.2690	0.3106	0.2671	0.3265	0.3224	0.2773	0.3251	0.3266	<b>0.3342</b>	<b>0.3460</b>	3.53%
	NDCG@40	0.0932	0.1529	0.1494	<b>0.1665</b>	0.1034	0.1309	0.1528	0.1325	0.1644	0.1619	0.1347	0.1622	0.1624	<b>0.1707</b>	<b>0.1783</b>	4.45%
Amazon-Electronics	Recall@20	0.1342	0.1319	0.1355	<b>0.1393</b>	0.1360	0.1254	0.0597	0.1255	0.1371	0.1295	<b>0.1377</b>	0.1306	0.1306	0.1311	<b>0.1407</b>	1.22%
	NDCG@20	0.0783	0.0792	0.0783	<b>0.0797</b>	0.0789	0.0727	0.0338	0.0742	0.0777	0.0748	<b>0.0803</b>	0.0771	0.0771	0.0792	<b>0.0812</b>	1.12%
	Recall@40	0.1873	0.1850	0.1955	0.1916	<b>0.1963</b>	0.1306	0.0918	0.1816	0.1939	0.1833	<b>0.1978</b>	0.1908	0.1907	0.1742	<b>0.2015</b>	1.87%
	NDCG@40	0.0933	<b>0.0958</b>	0.0948	0.0944	0.0954	0.0771	0.0426	0.0895	0.0934	0.0897	<b>0.0967</b>	0.0934	0.0934	0.0912	<b>0.0977</b>	1.03%
Amazon-CDs	Recall@20	0.1111	0.1572	0.1532	<b>0.1778</b>	0.1160	0.1510	0.0658	0.1309	0.1722	0.1430	0.1667	<b>0.1804</b>	0.1394	0.1443	<b>0.1823</b>	1.05%
	NDCG@20	0.0659	0.0981	0.0953	<b>0.1163</b>	0.0720	0.1000	0.0434	0.0815	0.1132	0.0862	0.1046	<b>0.1181</b>	0.0912	0.0929	<b>0.1202</b>	1.69%
	Recall@40	0.1695	0.2196	0.2141	<b>0.2401</b>	0.1678	0.2057	0.1076	0.1890	0.2319	0.2082	0.2333	<b>0.2418</b>	0.1940	0.1974	<b>0.2449</b>	1.28%
	NDCG@40	0.0821	0.1157	0.1124	<b>0.1338</b>	0.0886	0.1154	0.0542	0.0978	0.1230	0.1044	0.1231	<b>0.1353</b>	0.1066	0.1085	<b>0.1377</b>	1.77%
Tmall	Recall@20	0.0717	0.0737	0.0676	<b>0.1035</b>	0.0705	0.0730	0.0930	0.0706	0.0993	0.0880	0.0684	<b>0.1033</b>	0.0879	0.0879	<b>0.1040</b>	0.44%
	NDCG@20	0.0498	0.0515	0.0464	<b>0.0745</b>	0.0488	0.0511	0.0663	0.0492	<b>0.0712</b>	0.0626	0.0470	0.0626	0.0612	0.0612	<b>0.0753</b>	0.64%
	Recall@40	0.1126	0.1168	0.1059	<b>0.1545</b>	0.1104	0.1124	0.1427	0.1118	<b>0.1505</b>	0.1370	0.1082	0.1370	0.1379	0.1380	<b>0.1559</b>	0.86%
	NDCG@40	0.0640	0.0665	0.0598	<b>0.0922</b>	0.0626	0.0648	0.0834	0.0634	<b>0.0890</b>	0.0795	0.0607	0.0795	0.0784	0.0785	<b>0.0933</b>	0.85%

Table 3: Performance comparison to popular graph-based CF and CL models. We highlight the best 3 results in red (first), blue (second), and purple (third). *Imp.* stands for relative improvement over second-best performance. See *Appendix E* for Cohen’s effect size (Sullivan and Feinn 2012) results for statistical testing.

reaction-diffusion system to contrast the information from the different graph signals. However, SimGCL and LightGCL perform the CL training for their final embeddings only, overlooking their intermediate embeddings. This enables RDGCL to capture more diverse and complementary features from the graph structure.

RDGCL can be viewed as an extension of LT-OCF, a continuous-time generalization of LightGCN. RDGCL reduces to LT-OCF if the reaction term and CL are removed. In contrast, BSPM applies low-pass and high-pass filters to the interaction matrix sequentially and only once, while RDGCL integrates these processes iteratively as per Eq (7).

## 4 Experiments

### Experimental Environments

**Datasets and Baselines** We evaluate our model and baselines with 5 real-world benchmark datasets: Yelp, Gowalla, Amazon-Electronics, Amazon-CDs, and Tmall (Wang et al. 2019; He et al. 2020b; Harper and Konstan 2015). The detailed dataset statistics are presented in *Appendix C*. We compare our model with the 14 baselines with 4 categories:

- Graph-based CFs include LightGCN (He et al. 2020b), LT-OCF (Choi, Jeon, and Park 2021), HMLET (Kong et al. 2022), GF-CF (Shen et al. 2021), and BSPM (Choi et al. 2023a);
- Graph CL methods for other tasks include SimGRACE (Xia et al. 2022a) and GCA (Zhu et al. 2021);
- Hypergraph-based CFs include HCCF (Xia et al. 2022b) and SHT (Xia, Huang, and Zhang 2022);
- Graph CL methods for CF include SGL (Wu et al. 2021), SimGCL (Yu et al. 2022b), XSimGCL (Yu et al. 2022a), NCL (Lin et al. 2022), and LightGCL (Cai et al. 2023).

**Evaluation Protocols and Hyperparameters** We strictly follow evaluation protocols of Cai et al. (2023), using Recall@20/40 and NDCG@20/40. We use hyperparameters for all baseline models based on their recommended ranges. The detailed search ranges and the best settings for RDGCL on each dataset are provided in *Appendix D*.

### Experimental Results

Table 3 shows Recall@20/40 and NDCG@20/40. Our RDGCL clearly shows the highest accuracy in all cases. Specifically for Gowalla, RDGCL’s NDCG@20 is 5.19% higher than the best baseline. SGL and SimGCL perform well in some cases, with only SimGCL comparable to the accuracy of RDGCL on Yelp. SGL comparable to RDGCL on Tmall. However, the accuracy gap between RDGCL and SGL is still non-trivial. XSimGCL, known to be efficient and perform well, does not perform well on datasets we use.

To further verify the performance of RDGCL, we compare it with two other recently proposed methods. GF-CF and BSPM show good performance, occupying the 2nd and 3rd places for Yelp and Gowalla. However, no existing methods are comparable to our RDGCL for all datasets.

### Trade-off Among Recall, Coverage, and Novelty

We analyze the balanced nature of our model in terms of recall, coverage, and novelty. To provide a comprehensive evaluation, we use the harmonic means of recall with both coverage and novelty. The detailed formulation of these harmonic means is provided in *Appendix F*. Coverage (Herlocker et al. 2004) refers to the range of items that models can recommend, and novelty (Zhou et al. 2010) measures how unexpected the recommended items are compared to their global popularity.

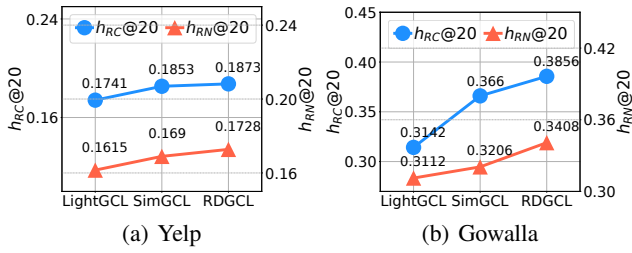


Figure 4: Trade-off among the three metrics

As shown in Fig. 4, LightGCL has low  $h_{RC}@20$  and  $h_{RN}@20$ , while RDGCL has the highest balanced performance. In the case of SimGCL, both metrics are lower than ours. This result suggests that RDGCL is a balanced design with improved accuracy and diversity.

### Robustness to Sparsity and Popularity Bias

To measure the robustness for sparse user groups, we divide users into three groups and measure Recall@20 for each group. The users were classified into three groups by interaction degree: the bottom 80%, from the bottom 80% to 95%, and the top 5%. As shown in Fig. 5, RDGCL consistently outperforms the other baselines for all groups of users. Specifically, RDGCL shows good accuracy for extremely sparse user groups ( $< 29$ ) in Gowalla.

Furthermore, we study the robustness to the item popularity bias with our method and the baselines. We divide items into three groups based on their degree of interaction and measure Recall@20 on each group  $g$ . Following SGL (Wu et al. 2021), we use the decomposed Recall@ $k$ , defined as  $\text{Recall}@k(g) = \frac{|(l_{rec}^u)^{(g)} \cap l_{test}^u|}{|l_{test}^u|}$ .  $l_{rec}^u$  represents the candidate items in the top- $k$  recommendation list and  $l_{test}^u$  represents the relevant items in the test set for user  $u$ .

Fig. 6 shows that the accuracy of our model is higher for the item group with a low interaction degree compared to other baselines. This indicates that our model recommends long-tail items and has the ability to alleviate popularity bias.

### Robustness to Noise Interactions

We evaluate the robustness of RDGCL and baselines to noise in user-item interactions. We add noise interactions randomly to the train dataset, train on the noisy train dataset, and evaluate it on the test dataset. We conduct by setting the percentage of random noise added to 0.1%, 0.3%, and 0.5% of the total number of interactions. Fig. 7 shows the performance of the models with respect to the noise ratio.

In the case of Yelp, the performance of SGL and LightGCL tends to decrease due to added noise interactions. In particular, SGL appears to be less robust to noise. However, we can see that our RDGCL and SimGCL still show high recommendation performance compared to other models.

### Ablation Studies

As ablation study models, we define 5 models: i) “RDGCL-EB” contrasts  $E(T)$  and  $B^{CL}$ , ii) “RDGCL-ES” contrasts

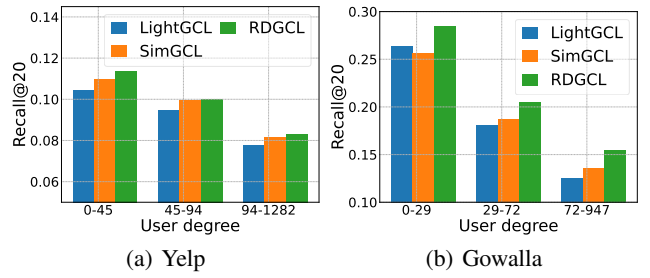


Figure 5: Performance on users of different sparsity degrees

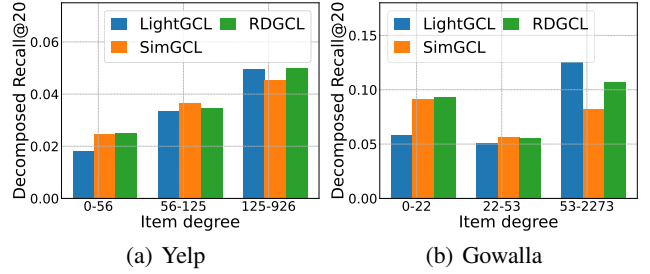


Figure 6: RDGCL’s ability to mitigate the popularity bias

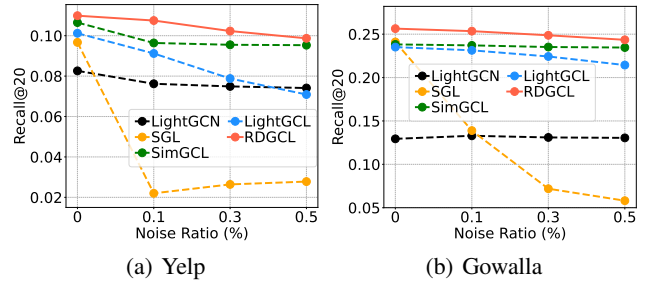


Figure 7: Recall@20 w.r.t. noise ratio

$E(T)$  and  $S^{CL}$ , iii) “w/o CL” removes  $\mathcal{L}_{CL}$ , iv) “Only Diffusion” uses only the diffusion term in Eq. (7), and v) “Only Reaction” uses only the reaction term in Eq. (7).

Table 4 shows the results on Yelp and Gowalla. RDGCL-ES outperforms RDGCL-EB, indicating the importance of the reaction process. The model without  $\mathcal{L}_{CL}$  shows a performance drop, underlining the role of CL in enhancing accuracy. Interestingly, “Only Diffusion” performs between SimGCL and LightGCL on Yelp, but still performs worse than RDGCL. “Only Reaction” fails to achieve complete alignment with RDGCL, highlighting the necessity of balancing both diffusion and reaction processes. These results validate the importance of each component in RDGCL.

### Empirical Evaluations for Oversmoothing

We analyze the oversmoothing (Oono and Suzuki 2020) in RDGCL and existing graph-based methods. Oversmoothing occurs when user/item node feature similarities converge to a constant value as the number of GCN layers increases. To measure oversmoothing, we use Dirichlet energy (Rusch,

Model	Yelp		Gowalla	
	Recall@20	NDCG@20	Recall@20	NDCG@20
RDGCL	0.1099	0.0939	0.2564	0.1549
RDGCL-EB	0.1024	0.0871	0.2495	0.1524
RDGCL-ES	0.1094	0.0935	0.2531	0.1530
w/o CL	0.0950	0.0794	0.1565	0.0929
Only Diffusion	0.1034	0.0878	0.2359	0.1388
Only Reaction	0.0875	0.0728	0.2266	0.1328

Table 4: Ablation studies on RDGCL

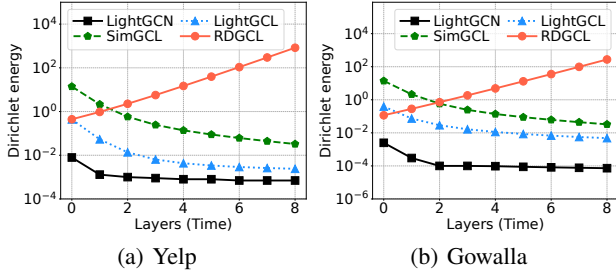


Figure 8: Evolution of the Dirichlet energy

Bronstein, and Mishra 2023). Fig. 8 shows the Dirichlet energy of final embeddings for various methods as the number of layers, while other methods show decrease of energy. This provides the resilience of RDGCL to oversmoothing, which can be attributed to its distinctive combination of low-pass and high-pass filters.

### Sensitivity Analyses

We conduct sensitivity analyses for RDGCL on key hyper-parameters: the terminal integral time  $T$ , the temperature  $\tau$ , the regularization weight for InfoNCE loss  $\lambda_1$ , and  $\alpha$ . The results for  $T$  and  $\alpha$  are presented in the main text, while the analyses for  $\tau$  and  $\lambda_1$  are in *Appendix H*.

**Sensitivity to  $T$**  We test the impact of the terminal integral time  $T$  of the reaction-diffusion process on our model, and the results are shown in Fig. 9.  $T$  close to 2 yields best results for both Yelp and Gowalla.

**Sensitivity to  $\alpha$**  Since the intensity of the high-pass filter is determined by  $\alpha$ , we test how our RDGCL accuracy changes by varying the reaction rate coefficient,  $\alpha$ , in Fig. 10. For Yelp, the best performance is shown when  $\alpha$  is near 0.6, while for Gowalla, the optimal coefficient is 0.2. It shows that the effect of CL is maximized at an optimal reaction rate coefficient for each dataset.

### Empirical Runtime Complexity

We also report our actual running time during training in Table 5. Our method does not involve augmentations on graph structures, and its single pipeline for CL is not separated from the main channel, unlike SGL and SimGCL. However, since RDGCL performs the reaction process, it has faster or comparable running times for some cases compared

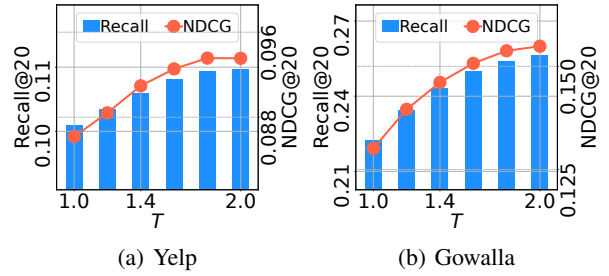


Figure 9: Sensitivity on  $T$

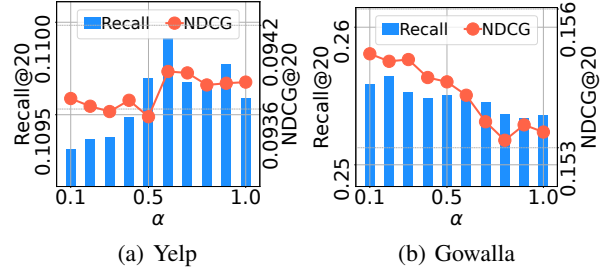


Figure 10: Sensitivity on  $\alpha$

Model	Yelp	Gowalla	Amazon- Electronics	Amazon- CDs	Tmall
SGL	44.91s	44.48s	19.58s	0.26s	102.55s
SimGCL	29.13s	50.02s	17.46s	0.25s	154.08s
XSimGCL	20.40s	38.37s	14.45s	0.21s	89.05s
LightGCL	19.94s	34.61s	11.81s	0.20s	90.59s
RDGCL	20.32s	34.89s	12.11s	0.20s	93.31s

Table 5: Efficiency comparison, w.r.t. the average training time per epoch

to XSimGCL and LightGCL. Nevertheless, our proposed method is still effective since it outperforms both XSimGCL and LightGCL by large margins in accuracy.

## 5 Conclusion & Limitation

We presented a novel approach called RDGCL for CF. It uses both the diffusion equation for low-pass filtering and the reaction equation for high-pass filtering in its design and CL training method. To the best of our knowledge, RDGCL is the first to adopt the reaction-diffusion equation for CL-based CF. In addition, our method is more efficient than other CL-based methods due to its *single pass* architecture. We demonstrated that RDGCL outperforms 14 baselines on 5 datasets and achieves the best-balanced performance among the recall, coverage and novelty.

Our limitation is that our reaction process requires another matrix multiplication computation in one layer. However, our single-pass architecture allows it to be efficient or comparable in runtime terms to other CL-based CF methods. Extending the reaction process to a more efficient one leaves for future work.

## References

- Allen, S. M.; and Cahn, J. W. 1979. A microscopic theory for antiphase boundary motion and its application to antiphase domain coarsening. *Acta metallurgica*, 27(6): 1085–1095.
- Bayer, M.; Kauffhold, M.-A.; and Reuter, C. 2022. A survey on data augmentation for text classification. *ACM Computing Surveys*, 55(7): 1–39.
- Cai, X.; Huang, C.; Xia, L.; and Ren, X. 2023. LightGCL: Simple Yet Effective Graph Contrastive Learning for Recommendation. In *ICLR*.
- Chamberlain, B. P.; Rowbottom, J.; Goronova, M.; Webb, S.; Rossi, E.; and Bronstein, M. M. 2021. GRAND: Graph Neural Diffusion. In *ICML*.
- Chen, L.; Wu, L.; Hong, R.; Zhang, K.; and Wang, M. 2020a. Revisiting Graph Based Collaborative Filtering: A Linear Residual Graph Convolutional Network Approach. In *AAAI*.
- Chen, R. T. Q.; Rubanova, Y.; Bettencourt, J.; and Duvenaud, D. K. 2018. Neural Ordinary Differential Equations. In *NeurIPS*.
- Chen, T.; Kornblith, S.; Norouzi, M.; and Hinton, G. 2020b. A Simple Framework for Contrastive Learning of Visual Representations. *arXiv preprint arXiv:2002.05709*.
- Chen, T.; Kornblith, S.; Swersky, K.; Norouzi, M.; and Hinton, G. 2020c. Big Self-Supervised Models are Strong Semi-Supervised Learners. *arXiv preprint arXiv:2006.10029*.
- Chen, T.; Luo, C.; and Li, L. 2021. Intriguing properties of contrastive losses. *NeurIPS*, 34: 11834–11845.
- Chen, Y.; and Pock, T. 2016. Trainable nonlinear reaction diffusion: A flexible framework for fast and effective image restoration. *IEEE transactions on pattern analysis and machine intelligence*, 39(6): 1256–1272.
- Choi, J.; Hong, S.; Park, N.; and Cho, S.-B. 2023a. Blurring-Sharpening Process Models for Collaborative Filtering. In *SIGIR*.
- Choi, J.; Hong, S.; Park, N.; and Cho, S.-B. 2023b. GREAD: Graph Neural Reaction-Diffusion Networks. In *ICML*.
- Choi, J.; Jeon, J.; and Park, N. 2021. LT-OCF: Learnable-Time ODE-based Collaborative Filtering. In *CIKM*.
- Chuang, Y.-S.; Dangovski, R.; Luo, H.; Zhang, Y.; Chang, S.; Soljagic, M.; Li, S.-W.; Yih, W.-t.; Kim, Y.; and Glass, J. 2022. DiffCSE: Difference-based Contrastive Learning for Sentence Embeddings. In *NAACL*.
- Chung, F. R. 1997. *Spectral graph theory*, volume 92. American Mathematical Soc.
- Du, X.; Yuan, H.; Zhao, P.; Qu, J.; Zhuang, F.; Liu, G.; Liu, Y.; and Sheng, V. S. 2023. Frequency Enhanced Hybrid Attention Network for Sequential Recommendation. In *SIGIR*, 78–88.
- Ekambaram, V. N. 2013. Graph Structured Data Viewed Through a Fourier Lens. *University of California, Berkeley*.
- Fan, W.; Liu, X.; Jin, W.; Zhao, X.; Tang, J.; and Li, Q. 2022. Graph Trend Filtering Networks for Recommendation. In *SIGIR*, 112–121.
- Fisher, R. A. 1937. The wave of advance of advantageous genes. *Annals of eugenics*, 7(4): 355–369.
- Harper, F. M.; and Konstan, J. A. 2015. The movielens datasets: History and context. *Acm transactions on interactive intelligent systems (tiis)*, 5(4): 1–19.
- Hassani, K.; and Khasahmadi, A. H. 2020. Contrastive multi-view representation learning on graphs. In *ICML*, 4116–4126. PMLR.
- He, K.; Fan, H.; Wu, Y.; Xie, S.; and Girshick, R. 2020a. Momentum contrast for unsupervised visual representation learning. In *CVPR*, 9729–9738.
- He, X.; Deng, K.; Wang, X.; Li, Y.; Zhang, Y.; and Wang, M. 2020b. LightGCN: Simplifying and Powering Graph Convolution Network for Recommendation. In *SIGIR*.
- Herlocker, J. L.; Konstan, J. A.; Terveen, L. G.; and Riedl, J. T. 2004. Evaluating Collaborative Filtering Recommender Systems. *ACM Trans. Inf. Syst.*, 22(1): 5–53.
- Hong, S.; Jo, M.; Kook, S.; Jung, J.; Wi, H.; Park, N.; and Cho, S.-B. 2022. TimeKit: A Time-series Forecasting-based Upgrade Kit for Collaborative Filtering. In *2022 IEEE International Conference on Big Data (Big Data)*, 565–574. IEEE.
- Hu, J.; Qian, S.; Fang, Q.; and Xu, C. 2022. MGDCF: Distance Learning via Markov Graph Diffusion for Neural Collaborative Filtering. *arXiv preprint arXiv: Arxiv-2204.02338*.
- Jaiswal, A.; Babu, A. R.; Zadeh, M. Z.; Banerjee, D.; and Makedon, F. 2020. A survey on contrastive self-supervised learning. *Technologies*, 9(1): 2.
- Jing, M.; Zhu, Y.; Zang, T.; and Wang, K. 2023. Contrastive Self-supervised Learning in Recommender Systems: A Survey. *arXiv preprint arXiv: Arxiv-2303.09902*.
- Khosla, P.; Teterwak, P.; Wang, C.; Sarna, A.; Tian, Y.; Isola, P.; Maschinot, A.; Liu, C.; and Krishnan, D. 2020. Supervised contrastive learning. *NeurIPS*, 33: 18661–18673.
- Kondo, S.; and Miura, T. 2010. Reaction-diffusion model as a framework for understanding biological pattern formation. *science*, 329(5999): 1616–1620.
- Kong, T.; Kim, T.; Jeon, J.; Choi, J.; Lee, Y.-C.; Park, N.; and Kim, S.-W. 2022. Linear, or Non-Linear, That is the Question! In *WSDM*, 517–525.
- Lee, Y.-C.; Kim, S.-W.; and Lee, D. 2018. gOCCF: Graph-theoretic one-class collaborative filtering based on uninteresting items. In *AAAI*, volume 32.
- Li, B.; Guo, T.; Zhu, X.; Li, Q.; Wang, Y.; and Chen, F. 2023. SGCCCL: siamese graph contrastive consensus learning for personalized recommendation. In *WSDM*, 589–597.
- Lin, Z.; Tian, C.; Hou, Y.; and Zhao, W. X. 2022. Improving graph collaborative filtering with neighborhood-enriched contrastive learning. In *TheWebConf (former WWW)*, 2320–2329.
- Liu, F.; Cheng, Z.; Zhu, L.; Gao, Z.; and Nie, L. 2021a. Interest-Aware Message-Passing GCN for Recommendation. In *TheWebConf (former WWW)*, 1296–1305.



- Liu, X.; Zhang, F.; Hou, Z.; Mian, L.; Wang, Z.; Zhang, J.; and Tang, J. 2021b. Self-supervised learning: Generative or contrastive. *IEEE Transactions on Knowledge and Data Engineering*, 35(1): 857–876.
- Mao, K.; Zhu, J.; Wang, J.; Dai, Q.; Dong, Z.; Xiao, X.; and He, X. 2021a. SimpleX: A Simple and Strong Baseline for Collaborative Filtering. In *CIKM*, 1243–1252.
- Mao, K.; Zhu, J.; Xiao, X.; Lu, B.; Wang, Z.; and He, X. 2021b. UltraGCN: Ultra Simplification of Graph Convolutional Networks for Recommendation. In *CIKM*.
- Nt, H.; and Maehara, T. 2019. Revisiting graph neural networks: All we have is low-pass filters. *arXiv preprint arXiv:1905.09550*.
- Oono, K.; and Suzuki, T. 2020. Graph neural networks exponentially lose expressive power for node classification. In *ICLR*.
- Oord, A. v. d.; Li, Y.; and Vinyals, O. 2018. Representation learning with contrastive predictive coding. *arXiv preprint arXiv:1807.03748*.
- Peng, S.; Sugiyama, K.; and Mine, T. 2022. Less is More: Reweighting Important Spectral Graph Features for Recommendation. In *SIGIR*, 1273–1282.
- Pinar, Z. 2021. An Analytical Studies of the Reaction-Diffusion Systems of Chemical Reactions. *International Journal of Applied and Computational Mathematics*, 7(3): 81.
- Plonka, G.; and Ma, J. 2008. Nonlinear regularized reaction-diffusion filters for denoising of images with textures. *IEEE Transactions on Image Processing*, 17(8): 1283–1294.
- Poli, M.; Massaroli, S.; Park, J.; Yamashita, A.; Asama, H.; and Park, J. 2019. Graph neural ordinary differential equations. *arXiv preprint arXiv:1911.07532*.
- Qiu, J.; Chen, Q.; Dong, Y.; Zhang, J.; Yang, H.; Ding, M.; Wang, K.; and Tang, J. 2020. GCC: Graph contrastive coding for graph neural network pre-training. In *KDD*, 1150–1160.
- Radford, A.; Kim, J. W.; Hallacy, C.; Ramesh, A.; Goh, G.; Agarwal, S.; Sastry, G.; Askell, A.; Mishkin, P.; Clark, J.; et al. 2021. Learning transferable visual models from natural language supervision. In *ICML*, 8748–8763. PMLR.
- Rusch, T. K.; Bronstein, M. M.; and Mishra, S. 2023. A Survey on Oversmoothing in Graph Neural Networks. *arXiv preprint arXiv: Arxiv-2303.10993*.
- Shen, Y.; Wu, Y.; Zhang, Y.; Shan, C.; Zhang, J.; Letaief, B. K.; and Li, D. 2021. How Powerful is Graph Convolution for Recommendation? In *CIKM*.
- Shin, Y.; Choi, J.; Wi, H.; and Park, N. 2023. An Attentive Inductive Bias for Sequential Recommendation Beyond the Self-Attention. *arXiv preprint arXiv:2312.10325*.
- Singer, A.; Shkolnisky, Y.; and Nadler, B. 2009. Diffusion interpretation of nonlocal neighborhood filters for signal denoising. *SIAM Journal on Imaging Sciences*, 2(1): 118–139.
- Sullivan, G. M.; and Feinn, R. 2012. Using effect size—or why the P value is not enough. *Journal of graduate medical education*, 4(3): 279–282.
- Turing, A. 1952. The chemical basis of morphogenesis. *Phil. Trans. R. Soc. Lond. B*.
- Turk, G. 1991. Generating textures on arbitrary surfaces using reaction-diffusion. *Acm Siggraph Computer Graphics*, 25(4): 289–298.
- Wang, X.; He, X.; Wang, M.; Feng, F.; and Chua, T.-S. 2019. Neural Graph Collaborative Filtering. In *SIGIR*.
- Wang, Y.; Wang, Y.; Yang, J.; and Lin, Z. 2021. Dissecting the Diffusion Process in Linear Graph Convolutional Networks. In *NeurIPS*.
- Wang, Y.; Yi, K.; Liu, X.; Wang, Y. G.; and Jin, S. 2023. ACMP: Allen-Cahn Message Passing for Graph Neural Networks with Particle Phase Transition. In *ICLR*.
- Witkin, A.; and Kass, M. 1991. Reaction-diffusion textures. In *Proceedings of the 18th annual conference on computer graphics and interactive techniques*, 299–308.
- Wu, J.; Wang, X.; Feng, F.; He, X.; Chen, L.; Lian, J.; and Xie, X. 2021. Self-Supervised Graph Learning for Recommendation. In *SIGIR*, 726–735.
- Xhonneux, L.-P. A. C.; Qu, M.; and Tang, J. 2020. Continuous Graph Neural Networks. In *ICML*.
- Xia, J.; Wu, L.; Chen, J.; Hu, B.; and Li, S. Z. 2022a. SimGRACE: A Simple Framework for Graph Contrastive Learning without Data Augmentation. In *TheWebConf (former WWW)*.
- Xia, L.; Huang, C.; Xu, Y.; Zhao, J.; Yin, D.; and Huang, J. 2022b. Hypergraph contrastive collaborative filtering. In *SIGIR*, 70–79.
- Xia, L.; Huang, C.; and Zhang, C. 2022. Self-supervised hypergraph transformer for recommender systems. In *KDD*, 2100–2109.
- Xu, Y.; Wang, Z.; Wang, Z.; Guo, Y.; Fan, R.; Tian, H.; and Wang, X. 2023. SimDCL: dropout-based simple graph contrastive learning for recommendation. *Complex & Intelligent Systems*, 1–13.
- You, Y.; Chen, T.; Sui, Y.; Chen, T.; Wang, Z.; and Shen, Y. 2020. Graph contrastive learning with augmentations. *NeurIPS*, 33: 5812–5823.
- Yu, J.; Gao, M.; Li, J.; Yin, H.; and Liu, H. 2018. Adaptive implicit friends identification over heterogeneous network for social recommendation. In *CIKM*, 357–366.
- Yu, J.; Xia, X.; Chen, T.; zhen Cui, L.; Hung, N. Q. V.; and Yin, H. 2022a. XSimGCL: Towards Extremely Simple Graph Contrastive Learning for Recommendation. *arXiv preprint arXiv:2209.02544*.
- Yu, J.; Yin, H.; Xia, X.; Chen, T.; Cui, L.; and Nguyen, Q. V. H. 2022b. Are graph augmentations necessary? simple graph contrastive learning for recommendation. In *SIGIR*, 1294–1303.
- Zhao, M.; Wu, L.; Liang, Y.; Chen, L.; Zhang, J.; Deng, Q.; Wang, K.; Shen, X.; Lv, T.; and Wu, R. 2022. Investigating accuracy-novelty performance for graph-based collaborative filtering. In *SIGIR*, 50–59.
- Zhou, H.; Chen, H.; Dong, J.; Zha, D.; Zhou, C.; and Huang, X. 2023. Adaptive popularity debiasing aggregator for graph collaborative filtering. In *SIGIR*, 7–17.

Zhou, T.; Kuscsik, Z.; Liu, J.-G.; Medo, M.; Wakeling, J. R.; and Zhang, Y.-C. 2010. Solving the apparent diversity-accuracy dilemma of recommender systems. *Proceedings of the National Academy of Sciences*, 107(10): 4511–4515.

Zhu, Y.; Xu, Y.; Yu, F.; Liu, Q.; Wu, S.; and Wang, L. 2020. Deep graph contrastive representation learning. *arXiv preprint arXiv:2006.04131*.

Zhu, Y.; Xu, Y.; Yu, F.; Liu, Q.; Wu, S.; and Wang, L. 2021. Graph contrastive learning with adaptive augmentation. In *TheWebConf (former WWW)*, 2069–2080.

# Appendix

## A Full Derivation of RDG Layer Filter

We provide the full derivation of the  $2\tilde{\mathbf{A}} - \tilde{\mathbf{A}}^2$  filter applied in the RDG Layer under Euler discretization with  $dt = 1$ ,  $T = 1$ , and  $\alpha = 1$ :

$$\begin{aligned} \mathbf{E}(T) &= \mathbf{E}(0) - \tilde{\mathbf{L}}\mathbf{E}(0) + \tilde{\mathbf{L}}\tilde{\mathbf{A}}\mathbf{E}(0) \\ &= \mathbf{E}(0) + (\tilde{\mathbf{A}} - \mathbf{I})\mathbf{E}(0) + (\mathbf{I} - \tilde{\mathbf{A}})\tilde{\mathbf{A}}\mathbf{E}(0) \quad (13) \\ &= (2\tilde{\mathbf{A}} - \tilde{\mathbf{A}}^2)\mathbf{E}(0). \end{aligned}$$

This derivation shows how the RDG layer applies the  $2\tilde{\mathbf{A}} - \tilde{\mathbf{A}}^2$  filter to the initial embedding  $\mathbf{E}(0)$ , resulting in the final embedding  $\mathbf{E}(T)$ .

## B Proof of Theorem 1

*Proof.* Let  $\gamma_i$  be an eigenvalue of  $\tilde{\mathbf{A}}$ . As noted in the paper,  $\gamma_i \in (-1, 1]$  for normalized adjacency matrices. The frequency response of the  $\tilde{\mathbf{A}}$  filter is  $g_1(\gamma_i) = \gamma_i$ , while the RDGCL filter has a frequency response of  $g_2(\gamma_i) = 2\gamma_i - \gamma_i^2$ . To compare these filters, we analyze the difference of their responses:

$$\begin{aligned} \Delta g(\gamma_i) &= g_2(\gamma_i) - g_1(\gamma_i) \\ &= 2\gamma_i - \gamma_i^2 - \gamma_i \\ &= \gamma_i(1 - \gamma_i). \end{aligned}$$

This difference function  $\Delta f(\gamma_i)$  forms a parabola in the interval  $[0, 1]$ , starting at zero when  $\gamma_i = 0$ , reaching a maximum value of 0.25 at  $\gamma_i = 0.5$ , and returning to zero at  $\gamma_i = 1$ . This behavior is consistent with the findings of Singer, Shkolnisky, and Nadler (2009).

In the context of graph signal processing with the normalized adjacency matrix  $\tilde{\mathbf{A}}$ , eigenvalues closer to 1 correspond to relatively higher-frequency signals, while those closer to 0 correspond to lower-frequency signals. The positive  $\Delta g(\gamma_i)$  in  $(0, 1)$  indicates that the RDGCL filter emphasizes higher frequency components more than the  $\tilde{\mathbf{A}}$  filter in this range.

Formally, we can state:

$$\forall \gamma_i \in (0, 1) : \Delta g(\gamma_i) > 0.$$

This property enables the RDGCL filter to selectively emphasize relatively higher-frequency signals while attenuating low-frequency signals. In contrast to the  $\tilde{\mathbf{A}}$  filter, which acts as a low-pass filter, the RDGCL filter provides a more balanced frequency response.

Therefore, we conclude that the RDGCL filter enhances relatively higher frequency components compared to the  $\tilde{\mathbf{A}}$  filter, particularly in the range  $\gamma_i \in (0.5, 1)$ , while still maintaining some low-pass characteristics.  $\square$

This property enables RDGCL to maintain a balance between preserving higher frequency details and some degree of smoothing, potentially leading to better performance in tasks that require both local and global information processing.

## C Details of Datasets

For Yelp and Gowalla, we use the data settings from Cai et al. (2023). For Amazon-Electronics and Amazon-CDs, we use the dataset settings used by Mao et al. (2021b). We provide the detailed dataset statistics in Table 6.

Dataset	#Users	#Items	#Interactions	Density
Yelp	29,601	24,734	1,374,594	0.188%
Gowalla	50,821	57,440	1,302,695	0.045%
Amazon-Electronics	1,435	1,522	35,931	1.645%
Amazon-CDs	43,169	35,648	777,426	0.051%
Tmall	47,939	41,390	2,619,389	0.132%

Table 6: Statistics of datasets

## D Details of Experimental Settings & Hyperparameters

For our method, we test the following hyperparameters:

- For solving the integral problem, we consider the Euler method;
- The number of steps  $K$  is in  $\{1, 2, 3\}$ , and the terminal time  $T$  is in  $\{1.0, 1.1, \dots, 3.0\}$ ;
- The reaction rate coefficient  $\alpha$  is in  $\{0.1, \dots, 1.0\}$ ;
- For fair comparison, we set the embedding sizes for all methods to 256;
- The learning rate (lr) is in  $\{1.0 \times 10^{-4}, 5.0 \times 10^{-4}, 1.0 \times 10^{-3}, 2.0 \times 10^{-3}, 3.0 \times 10^{-3}, 5.0 \times 10^{-3}, 1.0 \times 10^{-2}\}$ ;
- The temperature  $\tau$  in the InfoNCE loss is in  $\{0.1, 0.2, 0.4, 0.6, 0.8, 1.0, 2.0, 5.0\}$ ;
- The regularization weight for the InfoNCE loss  $\lambda_1$  is in  $\{0.01, 0.1, 0.2, 0.3, 0.4, 0.5\}$ ;
- The regularization weight  $\lambda_2$  is in  $\{1.0 \times 10^{-8}, 1.0 \times 10^{-7}, 1.0 \times 10^{-6}, 1.0 \times 10^{-5}, 5.0 \times 10^{-5}\}$ .

We perform a grid search within the above search range to get the best set of configurations from each dataset, which are as follows:

- In Yelp,  $K = 2$ ,  $T = 2$ ,  $D = 256$ , lr =  $5 \times 10^{-4}$ ,  $\alpha = 0.6$ ,  $\tau = 0.1$ ,  $\lambda_1 = 0.3$ , and  $\lambda_2 = 5 \times 10^{-5}$ .
- In Gowalla,  $K = 2$ ,  $T = 2$ ,  $D = 256$ , lr =  $1 \times 10^{-3}$ ,  $\alpha = 0.2$ ,  $\tau = 0.4$ ,  $\lambda_1 = 0.5$ , and  $\lambda_2 = 1e - 06$ .
- In Amazon-Electronics,  $K = 3$ ,  $T = 3$ ,  $D = 256$ , lr =  $1 \times 10^{-3}$ ,  $\alpha = 0.1$ ,  $\tau = 5.0$ , and  $\lambda_1 = 0.01$ .
- In Amazon-CDs,  $K = 2$ ,  $T = 2$ ,  $D = 256$ , lr =  $1 \times 10^{-3}$ ,  $\alpha = 0.1$ ,  $\tau = 0.2$ ,  $\lambda_1 = 0.2$ ,  $\lambda_2 = 1e - 7$ .
- In Tmall,  $K = 2$ ,  $T = 2$ ,  $D = 256$ , lr =  $1 \times 10^{-3}$ ,  $\alpha = 0.6$ ,  $\tau = 0.7$ ,  $\lambda_1 = 0.4$ ,  $\lambda_2 = 1e - 7$ .

RDGCL v.s.	Cohen’s d			
	Recall@20	NDCG@20	NDCG@20	NDCG@40
LightGCN	0.81*	1.20*	0.78*	1.17*
LT-OCF	0.42*	1.63*	0.40*	0.62*
HMLET	0.50*	1.71*	0.49*	0.78*
SGL	0.13	1.36*	0.14	0.23*
SimGRACE	1.02*	2.12*	1.01*	1.47*
GCA	0.70*	1.84*	0.86*	1.07*
HCCF	0.88*	1.88*	0.85*	1.04*
SHT	0.80*	1.93*	0.77*	1.13*
SimGCL	0.15	1.37*	0.15	0.27*
XSimGCL	0.39*	1.60*	0.34*	0.56*
LightGCL	0.16	1.37*	0.15	0.22*
GFCF	0.36*	1.54*	0.32*	0.48*
BSPM	0.28*	1.44*	0.32*	0.39*

Table 7: The effect size using Cohen’s d. \* means a small effect size greater than 0.2, and \* means a medium effect size greater than 0.5.

## E Statistical Test with Cohen’s Effect Size

To evaluate the performance of RDGCL against the baseline models in all datasets, we apply Cohen’s d to quantify the effect size (Sullivan and Feinn 2012). This standardized measure of the difference between two means shows that RDGCL outperforms the baseline in almost all cases across all datasets. Specifically, the Cohen’s d results indicate not only statistical significance, but also practical significance, indicating a real-world benefit of RDGCL over the baseline.

The effect size calculated using Cohen’s d range is ‘small’ for 0.2 and above, and ‘medium’ for 0.5 and above. In Table 7, the results show that the improvement in RDGCL performance in terms of NDCG@20, a key metric for recommendation systems, is statistically significant. However, compared to SGL and LightGCL, it fails to reach 0.2 in terms of Recall@20 by a small margin. However, we believe that our RDGCL is an attractive choice for improving recommendation algorithms, not only because of the accuracy of its recommendations, but also because of the novelty and diversity of the items it recommends, as shown in Sec. 4.

## F Harmonic Mean Formulation

To evaluate the balance between recall and other important metrics (coverage and novelty), we use the following two harmonic means:

$$h_{RC}@k = \frac{2 \times \text{Recall}@k \times \text{Coverage}@k}{\text{Recall}@k + \text{Coverage}@k}, \quad (14)$$

$$h_{RN}@k = \frac{2 \times \text{Recall}@k \times \text{Novelty}@k}{\text{Recall}@k + \text{Novelty}@k}, \quad (15)$$

where  $h_{RC}@k$  represents the harmonic mean of Recall and Coverage at top-k recommendations, and  $h_{RN}@k$  represents the harmonic mean of Recall and Novelty at top-k recommendations. These harmonic means provide a balanced measure of the model’s performance, considering both Recall and their diversity (i.e., Coverage and Novelty). By using these metrics, we can evaluate how well models bal-

ance these often competing objectives in recommendation systems.

## G Full Results for Robustness to Noise Interactions

We extend the results in the main content to evaluate the robustness of RDGCL and the baseline models to noise in user-item interactions and report on all metrics.

Tables 8 and 9 show the performance of the models with respect to the noise ratio. Our analysis reveals that RDGCL consistently outperforms all baseline models across different noise ratios (0.1%, 0.3%, 0.5%) on both datasets, showing its robustness for noisy interactions. As the noise ratio increases, we observe a general trend of performance degradation across all models, but RDGCL shows the least decline, indicating its superior noise resistance. Interestingly, on Yelp, the performance gap between RDGCL and SimGCL narrows slightly as noise increases, but RDGCL maintains its superiority.

On Gowalla, SGL appears most sensitive to noise, with significant performance drops as noise increases. SimGCL and LightGCL show intermediate robustness, but still underperform compared to our RDGCL.

Noise Metric	LightGCN	SGL	SimGCL	LightGCL	RDGCL	
0.1%	Recall@20	0.0762	0.0229	0.0964	0.0912	0.1075
	NDCG@20	0.0647	0.0191	0.0815	0.0752	0.0917
	Recall@40	0.1249	0.0550	0.1543	0.1467	0.1691
	NDCG@40	0.0827	0.0313	0.1026	0.0957	0.1141
0.3%	Recall@20	0.0749	0.0264	0.0955	0.0788	0.1023
	NDCG@20	0.0633	0.0215	0.0808	0.0643	0.0866
	Recall@40	0.1235	0.0417	0.1530	0.1310	0.1614
	NDCG@40	0.0812	0.0270	0.1016	0.0837	0.1083
0.5%	Recall@20	0.0741	0.0278	0.0953	0.0709	0.0987
	NDCG@20	0.0620	0.0218	0.0800	0.0580	0.0831
	Recall@40	0.1223	0.0461	0.1532	0.1187	0.1573
	NDCG@40	0.0797	0.0286	0.1011	0.0757	0.1045

Table 8: The results w.r.t. noise ratio on Yelp

Noise Metric	LightGCN	SGL	SimGCL	LightGCL	RDGCL	
0.1%	Recall@20	0.1329	0.1389	0.2363	0.2314	0.2535
	NDCG@20	0.0803	0.0568	0.1400	0.1360	0.1526
	Recall@40	0.1921	0.2412	0.3258	0.3222	0.3432
	NDCG@40	0.0957	0.0843	0.1635	0.1596	0.1761
0.3%	Recall@20	0.1310	0.0719	0.2352	0.2243	0.2487
	NDCG@20	0.0793	0.0317	0.1381	0.1314	0.1483
	Recall@40	0.1903	0.1426	0.3253	0.3109	0.3380
	NDCG@40	0.0948	0.0496	0.1617	0.1541	0.1719
0.5%	Recall@20	0.1305	0.0581	0.2346	0.2144	0.2435
	NDCG@20	0.0789	0.0270	0.1369	0.1256	0.1435
	Recall@40	0.1878	0.1097	0.3225	0.3001	0.3326
	NDCG@40	0.0939	0.0399	0.1601	0.1481	0.1671

Table 9: The results w.r.t. noise ratio on Gowalla

## H Sensitivity Analyses

**Sensitivity to  $\tau$**  We test our model for various settings of  $\tau$ , and the results are shown in Fig. 11. In Gowalla, performance improves as the value of  $\tau$  increases until reaching an optimal point around 0.4. As  $\tau$  becomes too large (e.g.,  $\tau \geq 0.5$ ), the performance decreases drastically in both datasets.

**Sensitivity to  $\lambda_1$**  We vary the regularization weight for the InfoNCE loss, denoted  $\lambda_1$ . The results are shown in Fig. 12. For both Yelp and Gowalla, the performance of our RDGCL increases rapidly as  $\lambda_1$  increases. After that, it shows slight decreases. However, the performance does not decrease as much as that of Fig. 11.

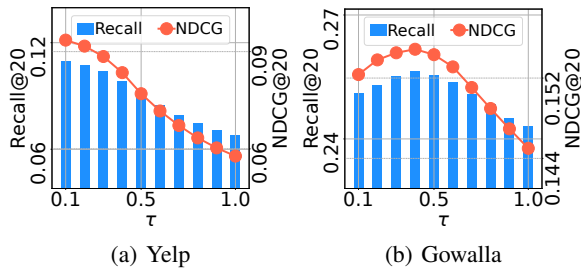


Figure 11: Sensitivity on  $\tau$

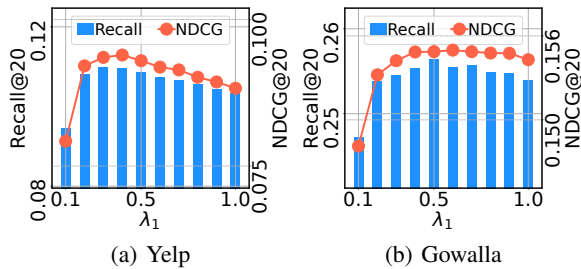


Figure 12: Sensitivity on  $\lambda_1$